

Application of Ceramic Plasma-Spray Coatings for Melting Crucible of Metallic Fuel

Ki-Won Hong^{a,b}, Ki-Hwan Kim^{b,*}, Sun-Ig Hong^a

^a Materials Science & Engineering, Chungnam National University, Daejeon, 34134, Republic of Korea

^b Next-Generation Nuclear Fuel Development Division, Korea Atomic Energy Research Institute, Daejeon, 34507, Republic of Korea

Corresponding author: khkim2@kaeri.re.kr (Ki-Hwan Kim)

1. Introduction

Research on the prevention of interaction has progressed since the 1990s because graphite crucible interacts with uranium alloy at high temperature, which causes a contamination of the fuel slugs [1-4]. Reaction testing of ceramic plasma-spray coated with U-10wt.%Zr-5wt.%RE has progressed to the evaluation of the protective performance of ceramic materials. Y_2O_3 , TaC, and TiC were selected as protective ceramic materials and sprayed onto graphite substrates [5-8]. Ceramic materials with a single coating layer and multiple coating layers were applied to the graphite rods. Interaction research progressed through a dipping test at 1470°C. SEM/EDS investigations were conducted to evaluate the micro-structural features of the coatings. Yttrium oxide and yttrium oxide on titanium carbide coating layers shows a better reaction resistance for U-10wt.%Zr-5wt.%RE melt.

2. Methods and Results

2.1 Experimental procedure

150 microns and 250 microns of a yttrium oxide layer were formed to investigate the effects of the thickness of a single layer. Titanium carbide and tantalum carbide layers were coated between the graphite substrate and yttrium oxide layer to investigate their effects as a conjugate coating layer. Finally, a tantalum carbide layer was applied to the substrate to judge the efficiency as a protective coating layer. All coating layers were applied using a plasma-spray coating method. The applied temperature cycle is shown in Fig. 1.

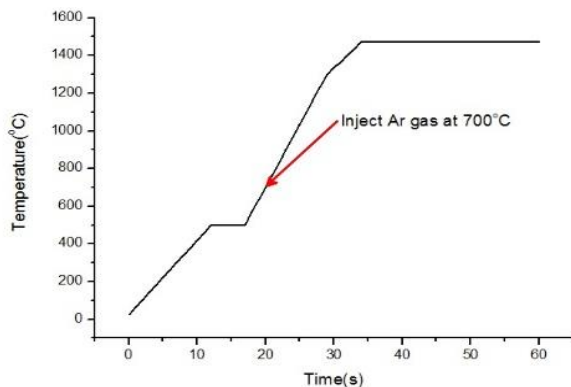


Fig. 1. Applied temperature cycle used to melt U-10wt.% Zr-5wt.%RE alloy.

2.2 Results

Photographs of the graphite rods after a dipping test are shown in Fig. 2. Tiny cracks from thermal expansion appeared at the top of the Y_2O_3 (150 μ m) and Y_2O_3 (250 μ m) specimens, but the specimens were generally fine. A slight attack by rare-earth elements was also shown in the TiC- Y_2O_3 and TaC- Y_2O_3 specimens. The sampling progressed at the marks shown in middle section and the boundary section in Fig. 2. The middle section was exposed to U-10wt.%Zr-5wt.%RE alloy, and the boundary section was exposed to a relatively larger amount of rare-earth elements, which floated based on the difference in density and immiscible property.

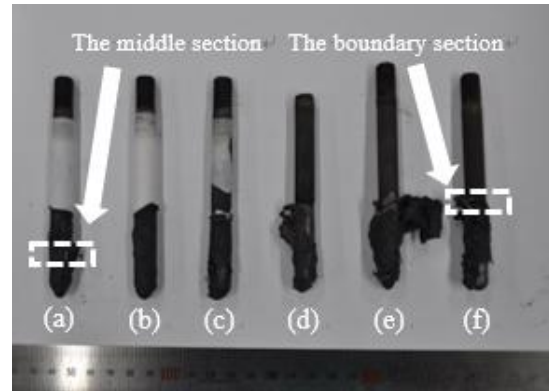


Fig. 2. Photographs of graphite rods after dipping test: (a) Y_2O_3 (150 μ m), (b) Y_2O_3 (250 μ m), (c) TaC- Y_2O_3 , (d) TiC- Y_2O_3 , (e) TaC, (f) TiC-TaC.

SEM micrographs of the middle section of the graphite rods with the coating materials are shown in Fig. 3. The coating layers of Y_2O_3 (150 μ m) for the specimen in Fig. 3 (a) were separated. On the other hand, separation was not detected in the Y_2O_3 (250 μ m) and TiC- Y_2O_3 specimens, and the coating layers remained relatively intact, although some cracks appeared from thermal shock. The coating layer in the TaC- Y_2O_3 specimen was perfectly separated and its own shape was not shown. Only the substrates were observed in the TaC and TiC-TaC specimens because the attached U-10wt.%Zr-5wt.%RE alloy on the coating layer was separated through the oxidation of the rare-earth elements.

SEM micrographs of the boundary section of the graphite rods based on the coating materials are shown in Fig. 4. The coating layers were separated but remained relatively intact without an infiltration of U-10wt.%Zr-5wt.%RE alloy in the Y_2O_3 (150 μ m), Y_2O_3 (250 μ m), and TiC- Y_2O_3 specimens. However, only the substrates were

observed because the coating layers were perfectly separated on the substrates through the oxidation of rare-earth elements of U-10wt.%Zr-5wt.%RE alloy.

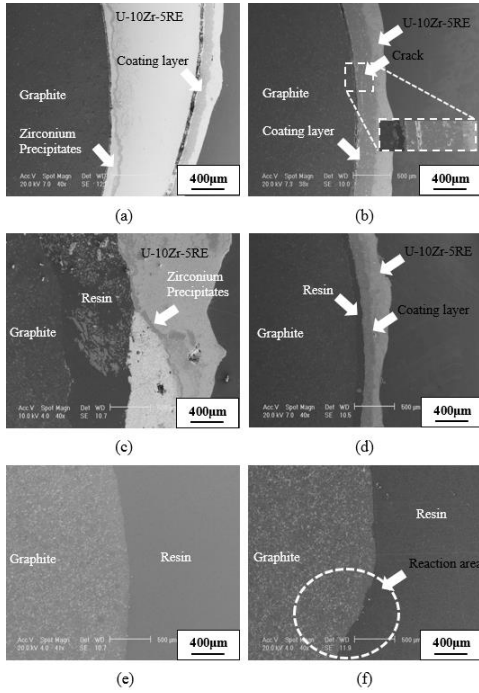


Fig. 3. SEM micrographs of the middle section of graphite rods based on the coating materials: (a) $Y_2O_3(150\mu m)$, (b) $Y_2O_3(250\mu m)$, (c) TaC- Y_2O_3 , (d) TiC- Y_2O_3 , (e) TaC, and (f) TiC-TaC.

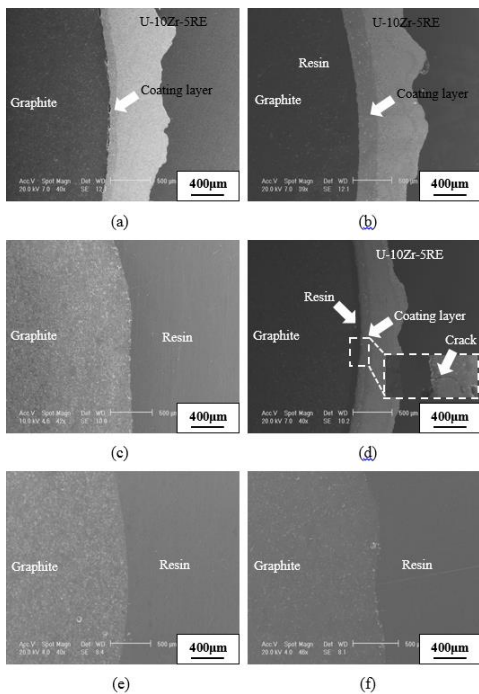


Fig 4. SEM micrographs of the boundary section of graphite rods based on the coating materials: (a) $Y_2O_3(150\mu m)$, (b) $Y_2O_3(250\mu m)$, (c) TaC- Y_2O_3 , (d) TiC- Y_2O_3 , (e) TaC, and (f) TiC-TaC.

Line scans of the cross-section of the middle section and the boundary section are shown in Figs. 5 and 6. A number of yttrium elements were detected in the yttrium oxide coating layer area, and carbon and uranium elements were detected in the left and right areas of the yttrium oxide coating layer area. Neodymium elements, which compose 53% of rare-earth alloys, were detected at the boundary area of the coating layer but were not detected inside of the coating layer. This is decisive evidence proving the performance of a yttrium oxide coating layer as a protective coating layer. A large number of rare-earth elements were detected more in the boundary section of the graphite rods than in the middle section through flotation based on the differences in the density and immiscibility of rare-earth elements.

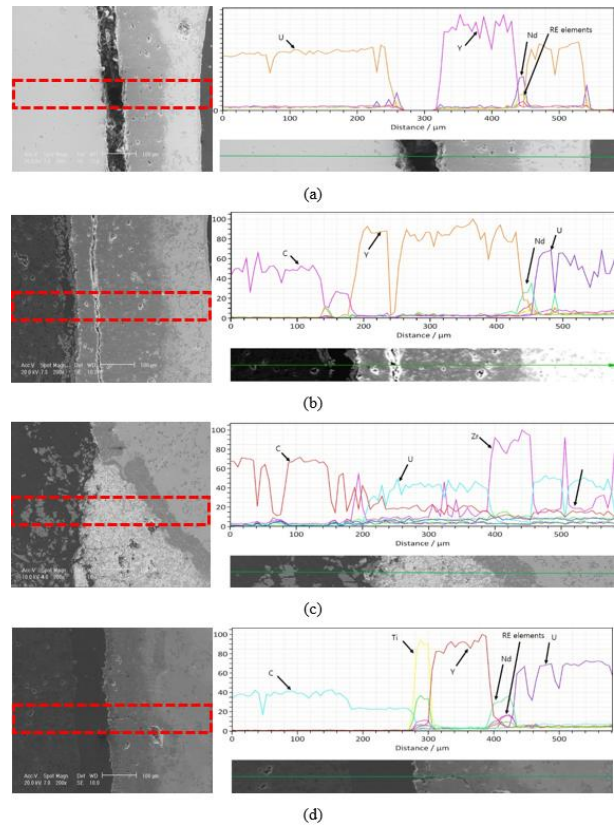
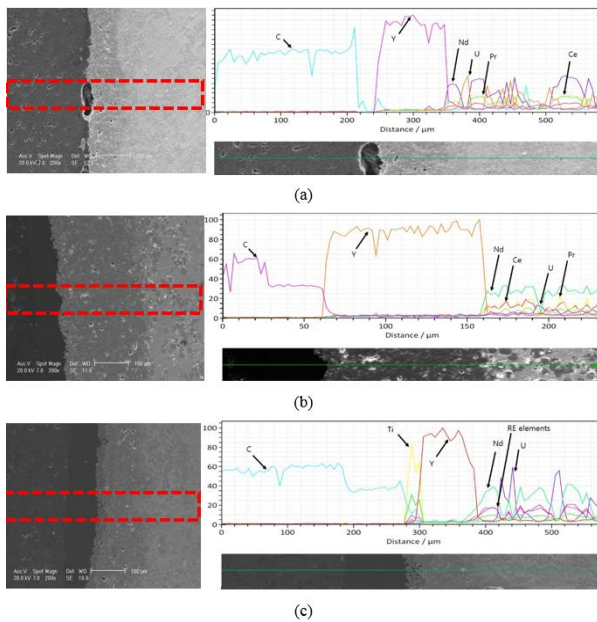


Fig. 5. Line scan of the cross-section of the middle section: (a) $Y_2O_3(150\mu m)$, (b) $Y_2O_3(250\mu m)$, (c) TaC- Y_2O_3 , and (d) TiC- Y_2O_3 .



[8] J.W. Koger, C.E. Holcombe, J.G. Banker, *Thin Solid Films*, 39 (1976) 297-303.

Fig 6. Line scan of the cross-section of the boundary section: (a) Y_2O_3 (150 μ m), (b) Y_2O_3 (250 μ m), and (c) TiC- Y_2O_3 .

3. Conclusions

The yttrium-oxide coating layer on a graphite substrate using plasma-spray coating method shows an excellent protection performance. However, the carbide coating materials do not show their own performance. It is thought that the Y_2O_3 coating layer showed good adhesion with few small pores owing to its relatively low melting temperature compared to carbide coating layers with melting temperatures in excess of 3100 °C. However, the flaking phenomenon still remains as a problem requiring a solution. It is possible to reuse the melting crucibles when resolving the flaking phenomenon.

REFERENCES

- [1] Robert B. Heimann, *Plasma Spray Coating, Principle and Applications*, Wiley-VCH, 1996.
- [2] L. Pawlowski, *The Science and Engineering of Thermal Spray Coatings*, John Wiley & Sons Ltd, Chichester, England, 1995.
- [3] X.Q. Cao, R. Vassen, D. Stoeber, *J. European Ceramic Society*, 24 (2004) 1-10.
- [4] E. Celika, I. Ozdemir, E. Avci, Y. Tsunekawa, *Surface & Coatings Tech.* 193 (2005) 297– 302.
- [5] Ki Hwan Kim, Chong Tak Lee, Chan Bock Lee, R.S. Fielding, J.R. Kennedy, *Journal of Nuclear Materials*, 2013.
- [6] Sung Ho Lee, Choon Ho Cho, Yoon Sang Lee, Han Soo Lee, Jeong-Guk Kim, *Korean, J. Chem. Eng.*, 27(6) (2010) 1786-1790.
- [7] Ki Hwan Kim, Chong Tak Lee, Chan Bock Lee, R.S. Fielding, J.R. Kennedy, *Thin Solid Films*, 519 (2011) 6969–6973.